Crack layer analysis of nonmonotonic fatigue crack propagation in high density polyethylene

K. Sehanobish, A. Moet and A. Chudnovsky
Department of Macromolecular Science, Case Western Reserve University, Cleveland, Ohio 44106, USA
(Received 21 October 1986; accepted 12 January 1987)

The rate of fatigue crack propagation (FCP) in high density polyethylene (HDPE) is a nonmonotonic function of the energy release rate, a phenomenon previously noted for other semicrystalline polymers. Microscopic observations reveal a single craze-like active zone preceding the crack during the initial crack acceleration. Subsequently crack deceleration is associated with a circular active zone. Ultimate failure occurs by crack reacceleration preceded by large scale yielding through an elongated damage zone accompanied by large scale deformation. Thus, FCP involves two mechanisms: quasibrittle and ductile. The former dominates the initial acceleration regime and the latter dominates subsequent nonmonotonic crack propagation. This anomalous crack propagation behaviour is well described by the 'crack layer' (CL) theory according to which the specific enthalpy of damage for the brittle and ductile mechanisms are found to be about 0.1 and 1 cal/g, respectively.
(Keywords: fatigue; crack; polyethylene; brittle; ductile; crack layer; energy release rate; specific enthalpy)

INTRODUCTION

Kinematic measurements of fatigue crack propagation in high density polyethylene (HDPE) shows that the rate of crack propagation does not increase monotonically as predicted by conventional laws of fracture mechanics. Specifically crack deceleration is clearly noticeable at well developed cracks. Such anomalous crack growth behaviour has been reported by several investigators[1-5]. Hertzberg and coworkers have described such behaviour in low-density polyethylene and commented that 'the fundamental reason for this behaviour remains unknown'[2]. Andrews *et al.* concluded from their fracture surface analysis that the process involves two distinct regions of microbrittle and microductile crack propagation linked by a transition zone[1]. However, no attempt was made to describe crack propagation kinetics in this transition zone, i.e. the deceleration region. Recently, Chudnovsky *et al.* suggested that, in polypropylene, such anomalous behaviour is controlled by the damage dissemination ahead of the crack tip[4].

In this paper the crack layer approach is employed to quantitatively describe the nonmonotonic crack propagation behaviour in HDPE.

EXPERIMENTAL

The material used in this investigation is Marlex 6006 high density polyethylene resin supplied in bead form by Phillips Petroleum Company. The density of the material is 0.964 g cm^{-3}, $MFI = 0.75$, $\bar{M}_w = 130\,000$ and $\bar{M}_n = 19\,600$. The specimens were made from 0.6 mm thick compression moulded plaques prepared by slow cooling from the melt. Standard tensile tests showed that the Young modulus (E) is 1.1 GPa while the yield stress is approximately 30 MPa.

Straight notches of depth 1 mm were introduced into rectangular specimens of gauge dimension (20×80) mm. Fatigue tests were conducted at room temperature on a MTS servohydraulic machine using a sinusoidal wave form of frequency 0.5 Hz. Tension–tension loading was used with a maximum stress of 7.5 MPa and load ratio $R = 0.5$. The crack and the surrounding damage are simultaneously observed using a travelling optical microscope attached to a video camera assembly equipped with a visual display unit. Hysteresis loops associated with fatigue cycles are recorded during the entire experiment.

RESULTS

In *Figure 1* the rate of crack propagation ($\log dl/dN$) is presented as a function of crack length for three identical specimens. In spite of small variations in crack speed which are inevitable in fracture experiments, the data shows good reproducibility. The crack initially propagates at high monotonic acceleration, then decelerates reaching a plateau and finally reaccelerates towards rupture. Similar crack deceleration behaviour has been reported earlier in low density polyethylene[1,2]. Creep crack growth experiments conducted in our laboratory under comparable mean load level display similar three-stage crack propagation kinetics[6]. However, the crack deceleration region is less pronounced in creep and the failure occurs over a longer time scale.

To understand the reason for such crack propagation behaviour, the micromechanisms of crack propagation have been examined. *Figures 2a, b* and *c* show typical micrographs, sampled from video playbacks, of crack propagation. The spacing between the vertical lines is 1 mm. During the initial crack acceleration region (*Figure 2a*) the crack propagates preceded by an elongated active zone (white zone ahead of the crack tip). The general

0032-3861/87/081315-06$03.00

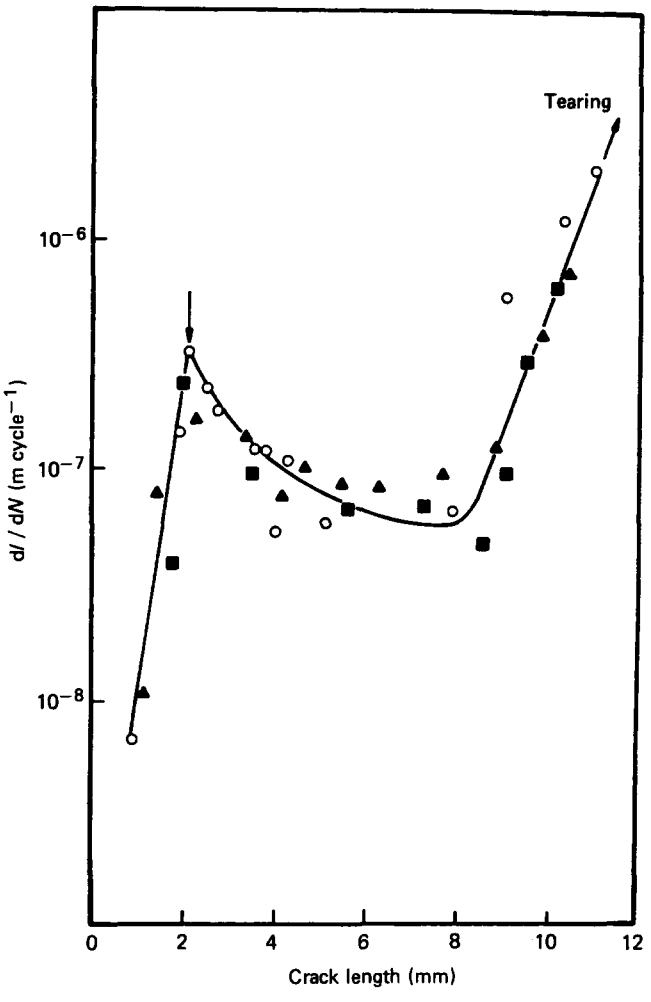

Figure 1 Crack speed dl/dN plotted as a function of crack length. The vertical arrow indicates the onset of crack deceleration

configuration of the active zone is reminiscent of a single craze crack growth, however, the zone size is orders of magnitude larger than a single craze[7]. A single craze mechanism dominates up to a crack length of 3.0 mm. The active zone is subsequently transformed into a circular configuration (*Figure 2b*) and maintains its circular shape during the entire crack deceleration region. Finally, the active zone elongates again during the last stage of crack reacceleration. Large voids develop within the active zone and the crack propagates through them. Ultimate failure occurs by a tearing process involving large scale flow at a crack length of 11.3 mm. From these observations, it is suggested that the active zone propagates by two dominant mechanisms, i.e. brittle-like (single craze) followed by large scale deformation. Crack deceleration occurs when the latter becomes predominant. This qualitatively agrees with Andrew's explanation of the transition from microbrittle to microductile crack propagation. However, we may encounter materials like polypropylene where crack deceleration involves an abrupt change in active zone shape rather than the damage mechanism[4]. Further evidence of the presence of two dominant mechanisms is obtained from the extent of yielding within the active zone. This is achieved from measurements of thinning (yielding) of the fracture surface. Dimensionless fracture surface thickness is plotted as a function of crack length in *Figure 3*. Once again we notice that up to about 3 mm (arrow in *Figure 3*), the thickness remains practically unchanged and then gradually decreases to about 40% of the initial material thickness.

The material resistance to crack propagation is manifested through evolution of damage ahead of the

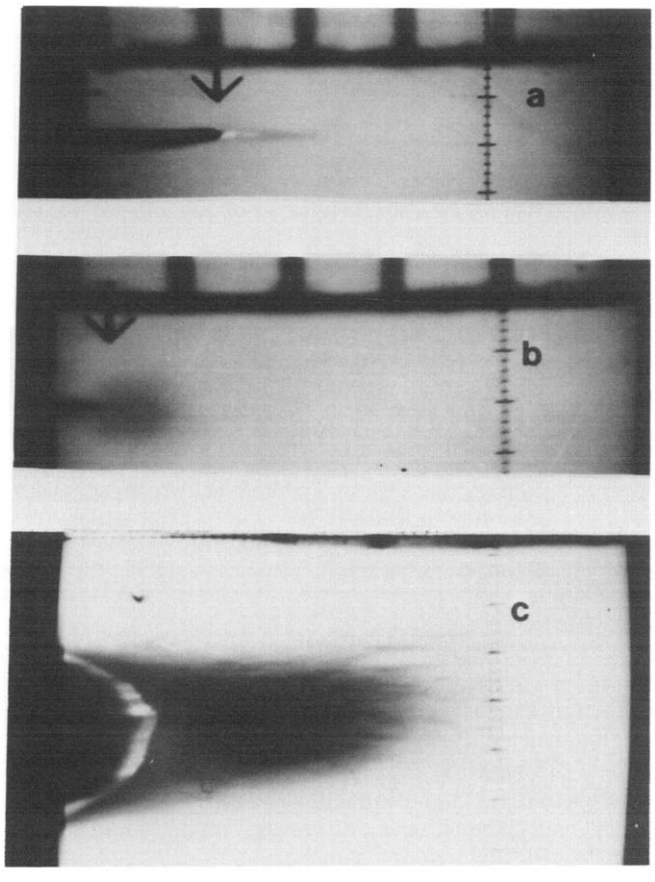

Figure 2 (a) Crack preceded by a single craze-like damage zone in the initial monotonic crack acceleration region. (b) Crack preceded by a circular damage zone in the crack deceleration region. (c) Crack preceded by an elongated damage zone in the final reacceleration region prior to tearing

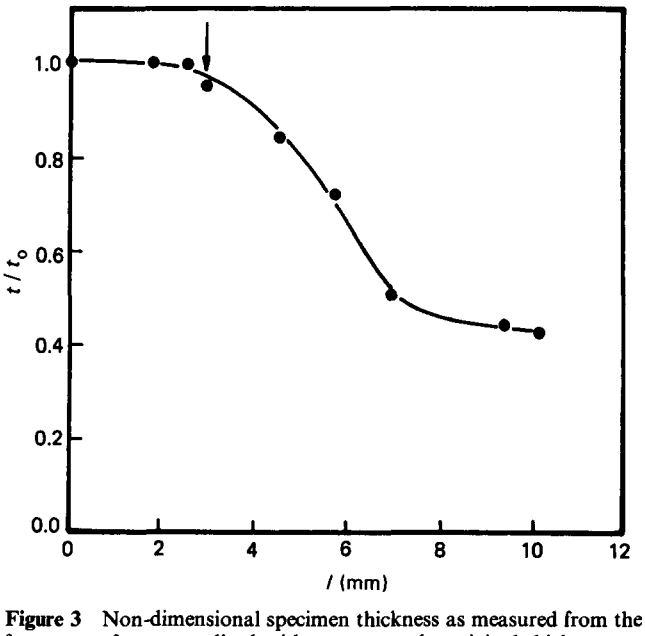

Figure 3 Non-dimensional specimen thickness as measured from the fracture surface normalized with respect to the original thickness vs. crack length

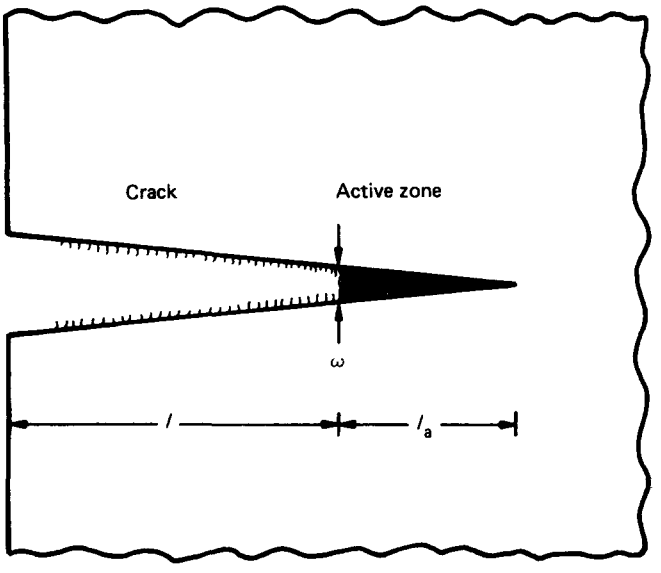

Figure 4 Schematic of a single craze-like damage zone in the brittle regime

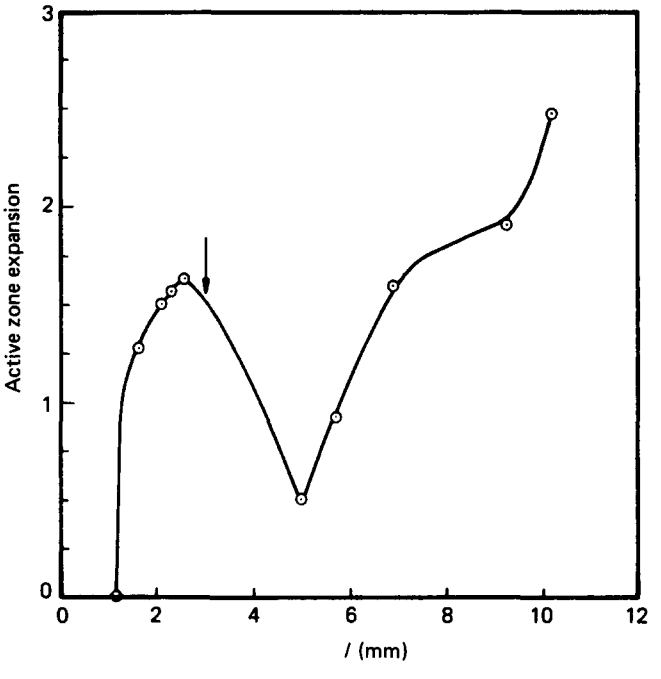

Figure 5 Active zone expansion e vs. crack length

crack tip (active zone). A measure of active zone evolution can be achieved through changes in its dimensions. *Figure 4* shows a schematic of an active zone which is characterized by its length l_a and width ω. Accordingly, the rate of the active zone deformation can be expressed by the following terms or (in cartesian coordinates):

$$\dot{d}=\begin{pmatrix} \dot{l}_a/l_{a0} & 0 & 0 \\ 0 & \dot{\omega}/\omega_0 & 0 \\ 0 & 0 & \dot{t}/t_0 \end{pmatrix} \tag{1}$$

where t is the fracture surface thickness and l_{a0}, ω_0, t_0 are the initial values of the active zone dimensions. The rate of isotropic expansion of the active zone '$\dot{e}$' is the spherical component of relation (1), i.e.

$$\dot{e}=\left(\frac{\dot{l}_a}{l_{a0}}+\frac{\dot{\omega}}{\omega_0}+\frac{\dot{t}}{t_0}\right) \tag{2}$$

while its distortion (shape change) is described by the second invariant of the deviatoric part of the rate of deformation expressed as

$$\dot{I}_d=\tfrac{1}{6}\left[\left(\frac{\dot{l}_a}{l_{a0}}\right)^2+\left(\frac{\dot{\omega}}{\omega_0}\right)^2+\left(\frac{\dot{t}}{t_0}\right)^2\right]^{1/2} \tag{3}$$

Expansion and distortion parameters (e and I_d) obtained as time integrals of equations (2) and (3) are plotted as a function of crack length in *Figures 5* and *6*. A transition in the active zone expansion (indicated by the arrow in *Figure 5*) is noticeable around the same crack length where crack deceleration begins (*Figure 1*).

DISCUSSION

The results clearly indicate that the rate of crack propagation is controlled by damage evolution within the active zone. Accordingly, the crack layer theory expresses the rate of crack propagation as[8]

$$\frac{dl}{dN}=\frac{dD/dN}{\gamma^* R_1-J_1} \tag{4}$$

where l and N are the crack length and number of cycles, respectively. D represents the energy dissipated on damage creation within the active zone, γ^* is the specific enthalpy of damage, R_1 is the resistance moment and J_1 is the potential energy release rate. Physically, R_1 can be identified with the total amount of material transformed within the active zone in resistance to propagation.

It has already been pointed out that the initial monotonic crack acceleration regime (*Figure 1*) is associated with a single craze type damage zone (*Figure 2a*)

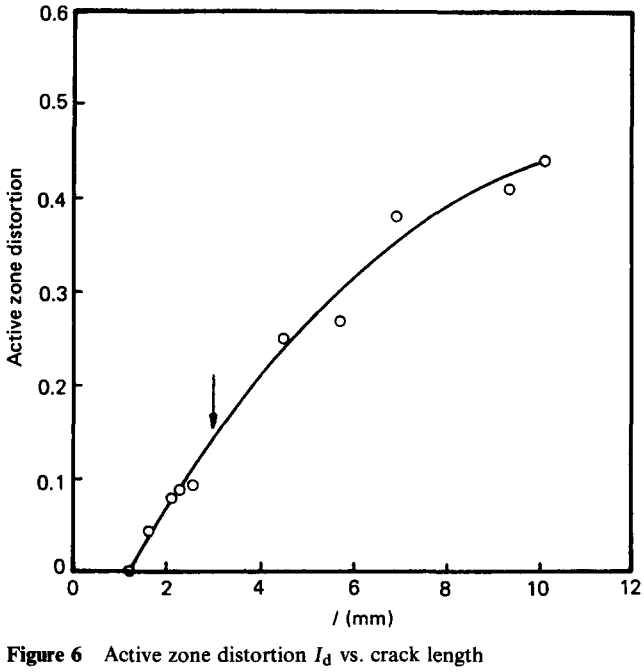

Figure 6 Active zone distortion I_d vs. crack length

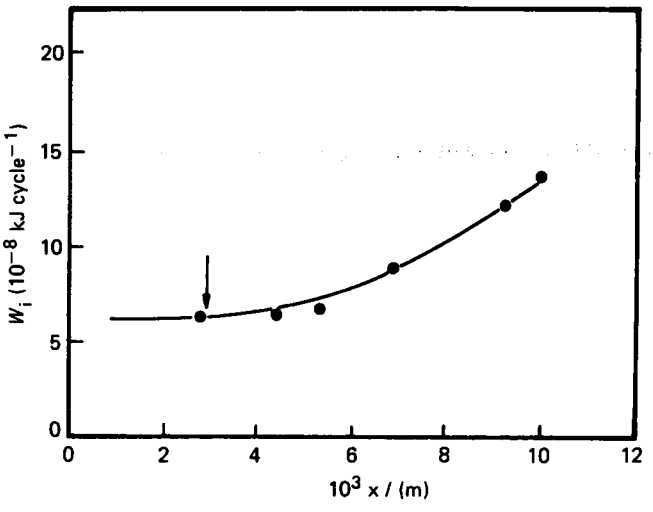

Figure 7 Irreversible work per cycle W_i as a function of crack length

reminiscent of brittle fracture. At a crack length of about 3 mm the damage mechanism transforms into profuse thinning and voiding typical of ductile fracture. Since fracture involves two dominant mechanisms, and that γ^* describes the specific enthalpy associated with a particular mechanism, it is therefore reasonable to analyse the two crack propagation regimes separately. In the following discussion we outline the procedures for evaluation of the parameters involved, i.e. D, R_1 and J_1. Thus from equation (4), the material parameter γ^* characteristic for each of the observed mechanisms is extracted.

Energy dissipation rate

The energy dissipation rate dD/dN, the numerator of equation (4), is a part, β, of the irreversible work W_i per unit cycle. W_i is obtained by subtracting the area within the load–displacement hysteresis loop prior to crack initiation from the hysteresis area corresponding to a specific crack length. *Figure 7* presents the plot of W_i in kJ/cycle as a function of crack length. It is clear that in the brittle regime, W_i appears virtually unchanged. Since the total displacement is very small in this regime, changes in W_i are anticipated to be too small to be detected by current instrumentation.

Indeed, crazing leads to irreversible deformation which is manifested on the macroscopic level as viscoelastic behaviour. Thus, we assume that the rate of energy dissipation on craze formation and growth within the active zone is proportional to part of the total potential energy associated with the active zone. In general, this potential energy can be expressed in terms of the energy release rate associated with expansion and distortion of the active zone, i.e. M and N integrals. Since this task is beyond the scope of this work, and in view of the fact that M and N are proportional to $l_a J_1$[9], dD/dN in the quasibrittle regime is approximated as $\beta' l_a J_1$.

Resistance moment

In general, the resistance moment R_1 is defined as the integral amount of damage formed per unit crack extension. Although microscopic analysis of the damage zone in HDPE in the ductile regime indicates fibrillation and voiding as secondary damage mechanisms apart from homogenous yielding[6]. In this paper R_1 will be crudely approximated based on the active zone size alone. Thus R_1 is calculated from the area increment of the active zone measured from the side view traced from video play backs (*Figures 2a, b, c*) and the extent of yielding measured from the fracture surface (*Figure 3*). A plot of R_1, in mm^3 of transofrmed material per unit crack extension in mm^2, as a function of crack length is presented in *Figure 8*. Again, changes in R_1 during the brittle regime appear to be too small to be detected at the scale of our observation. However, a considerable increase in R_1 is noted during the ductile regime.

Energy release rate

In the brittle regime, the active zone size is relatively small with respect to the crack length. Therefore $G_1 = K_I^2/E$ suffices as a measure of the energy release rate. However, in the ductile regime (*Figures 2b,c*) the active zone is relatively large. The elastic solution of the energy release rate is no longer applicable. Known elastoplastic solutions are not applicable either since the predicted plastic zone shape and size are essentially different from the zone observed. Therefore, the energy release rate is evaluated experimentally using conventional techniques based on evolution of the load–displacement curves[11].

Experimental determination of J_1 requires estimation of the area between the loading or unloading curves corresponding to the crack length increment. Usually, it is more instructive to consider the unloading curves rather than the loading curves for such measurements, since unwarranted crack propagation may occur during the loading excursion. However, in polyethylene significant cyclic creep contribution during fatigue crack propagation results in overestimation of this area. *Figure 9* explains the above situation schematically. Actual loading and unloading are shown by the solid lines, while the broken lines represent hypothetical paths traced by elastic loading and unloading. Thus, the shaded areas constitute the creep contribution. Observations of the permanent set, i.e. the permanent displacement of the ends of unloading curves at σ_{min} suggest the creep contribution during unloading is of the order of one half the cyclic displacement. Accordingly, 'elastic' unloading curves similar to that observed in *Figure 9* are reconstructed for energy release rate evaluation. The area dS between two such unloading curves provides a measure

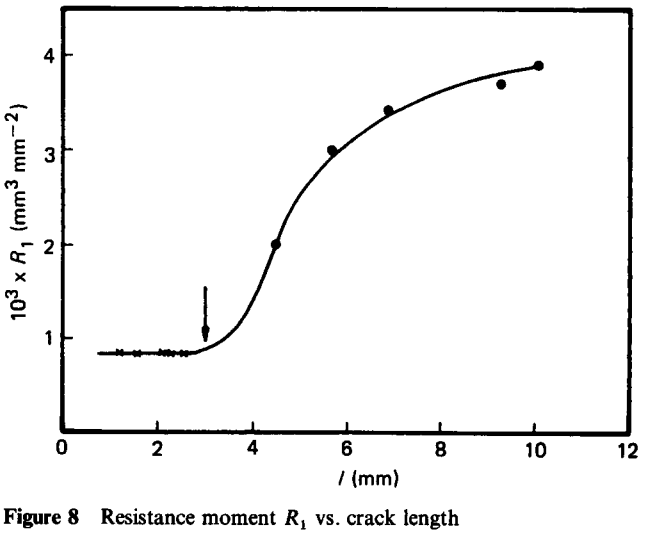

Figure 8 Resistance moment R_1 vs. crack length

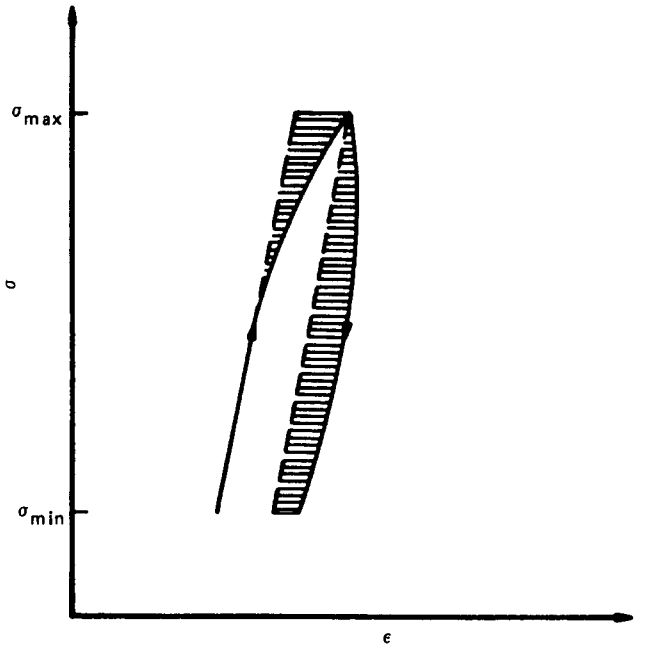

Figure 9 Schematic of cyclic stress–strain behaviour. The solid lines represent the actual loading–unloading behaviour whereas the broken lines indicate elastic loading and unloading, respectively. The shaded zones display the cyclic creep contribution during loading and unloading

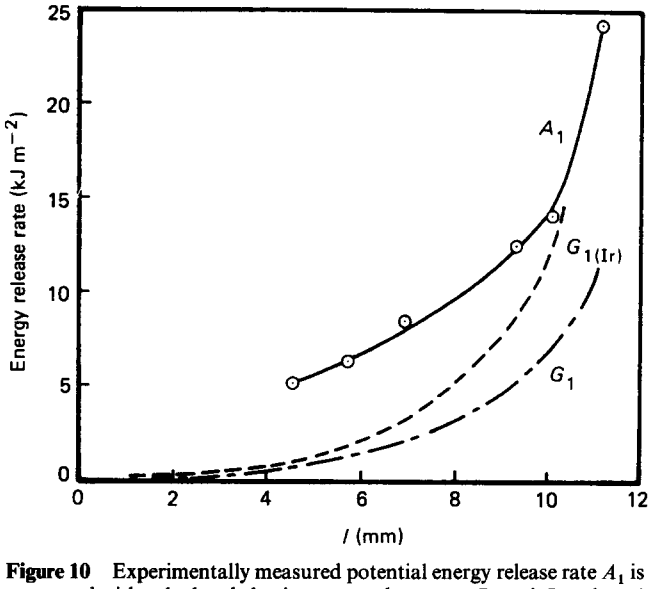

Figure 10 Experimentally measured potential energy release rate A_1 is compared with calculated elastic energy release rate G_1 and $G_{1(Ir)}$ based on Irwin's plastic zone correction

of the energy released due to crack layer extension from l_1 to l_2, i.e.

$$J_1 = -\frac{1}{t_o}\frac{dS}{l_2 - l_1} \tag{5}$$

where t_o is the original thickness of the specimen.

The elastic energy release rate G_1 based on the actual crack length and $G_{1(Ir)}$ based on the effective crack length are also calculated for comparison. Here the effective crack length is evaluated using Irwin's plastic zone correction[12]. Furthermore, it should be noted that the measured energy release rate contains the energy released due to active zone translation which coincides with J_1, and the energy released due to active zone deformation. Thus, to distinguish between the total energy release rate and the conventionally used translational energy release rate J_1, we assign the former as A_1[13]. A_1, G_1 and $G_{1(Ir)}$ are plotted as a function of crack length in *Figure 10*. We notice that in the ductile regime active zone deformation is significant (*Figures 5* and *6*) resulting in A_1 being larger than the predicted G_1 or $G_{1(Ir)}$. Finally the above parameters are employed to extract the specific enthalpy of damage γ^* and the phenomenological coefficients β' and β for each of the involved mechanisms. For this purpose, equation (4) can be rearranged as

$$\frac{G_1}{R_1} = -\beta' \frac{l_a G_1}{\frac{dl}{dN} R_1} + \gamma^* \tag{6}$$

for the brittle regime, and as

$$\frac{A_1}{R_1} = -\beta \frac{W_i}{t\frac{dl}{dN} R_1} + \gamma^* \tag{7}$$

for the ductile regime. In spite of the crudeness involved in data aquisition and analysis, the results are in reasonable agreement with the proposed relationship (*Figures 11* and *12*), particularly in the brittle regime.

The specific enthalpy of craze like damage is about 400 kJ/m^3 whereas that for large scale ductile damage is in the neighbourhood of 4000 kJ/m^3. These values can be roughly estimated as $\gamma^* \approx 0.1$ cal/g for craze like ('brittle') damage and $\gamma^* \approx 1$ cal/g for ductile damage. The first may be compared with 15 cal/g for polystyrene[10] and the second may be compared with 10 cal/g for commercial polycarbonate sheet[14]. The phenomenological coefficients β' and β are 1.6×10^{-5} cycle^{-1} and 0.002, respectively, whereas $\beta \approx 0.002$ indicates the portion of

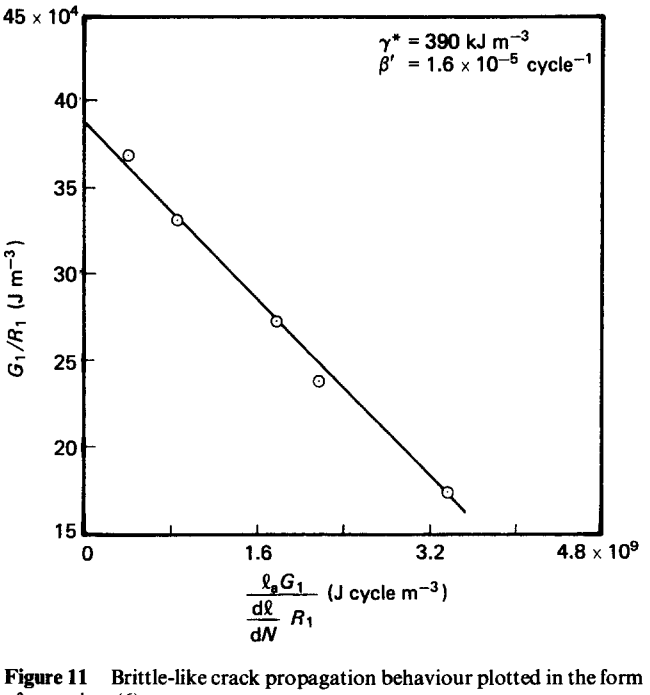

Figure 11 Brittle-like crack propagation behaviour plotted in the form of equation (6)

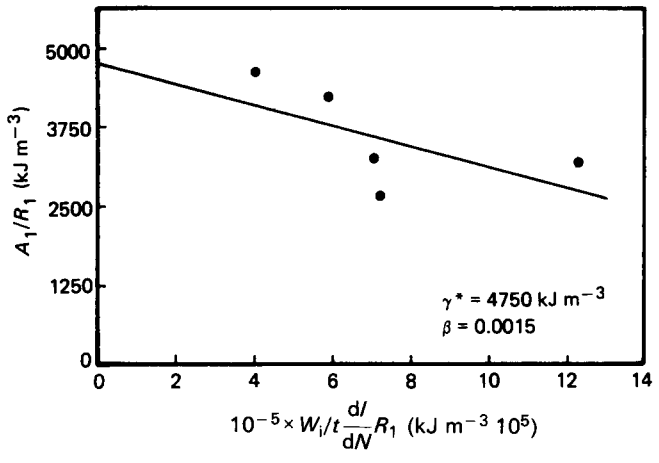

Figure 12 Ductile crack propagation behaviour plotted in the form of equation (7)

irreversible work done on damage formation and growth within the active zone, the physical meaning of β' remains unclear. The small value of β is understandable in view of the physical nature of irreversible deformation and fracture in polyethylene.

CONCLUSIONS

(1) Fatigue crack propagation in HDPE involves two competing mechanisms: craze like and large scale yielding. The first dominates during the initial monotonic crack propagation regime, and the second dominates crack deceleration and subsequent monotonic crack acceleration towards ultimate failure.

(2) The crack layer theory provides a reasonable description for the entire FCP history including crack deceleration. The specific enthalpy of damage for both processes are evaluated together with the dissipative parameters associated with damage evolution.

CLOSING REMARKS

The material (HDPE) exhibits strong time dependency which is more pronounced in the active zone due to high stress concentration. A clear manifestation of this effect is noticeable in the load–displacement hystrersis, as well as in large scale fibrillation and void formation. In the present analysis, we employed the evolution of load–displacement curves (*Figure 9*) for energy release rate evaluation assuming elastic response. In addition, the volume of the active zone as a measure of damage to evaluate the resistance moment. A more adequate description of the phenomenon requires viscoelastic analysis of the load–displacement curves and more detailed characterization of damage density. In view of this, the reported values for the specific enthalpy of damage ought to be considered as a tentative estimate.

ACKNOWLEDGEMENTS

The authors acknowledge the financial support of the Gas Research Institute, Grant No. 5083-260-0940.

REFERENCES

1 Andrews, E. H. and Walker, B. J. *Proc. Roy. Soc. Lond.* (*A*) 1971, **325**, 57
2 Bretz, P. E., Hertzberg, R. W. and Manson, J. A. *Polymer* 1981, **22**, 575
3 Sandt, A. and Hronbogen, E. *J. Mater. Sci. Lett.* 1981, **16**, 2915
4 Bankert, R. J., Takemori, M. T., Chudnovsky, A. and Moet, A. *J. Appl. Phys.* 1983, **14**, 5562
5 Morelli, T. A. and Takmori, M. T. *J. Mater. Sci.* 1984, **19**, 385
6 Kasakevich, M. L., Moet, A., Chudnovsky, A., Sehanobish, K. and Chaoui, K. GRI report, April, 1986
7 Doell, W. in 'Advances in Polymer Science', 52/53 (Ed. H. H. Kausch), Springer, Berlin–Heidelberg, 1983, p. 105
8 Chudnovsky, A. NASA report No. 174634, 1984
9 Sehanobish, K., Botsis, J., Moet, A. and Chudnovsky, A. *Int. J. Fract.* 1986, **32**, 21
10 Botsis, J., Chudnovsky, A. and Moet, A. *Int. J. Fract.* 1987, in press
11 Begley, J. A. and Landes, J. D. in 'Fracture Toughness', ASTM STP514, American Society for Testing and Materials, 1972, pp. 1–39
12 Broek, D. 'Elementary Engineering Fracture Mechanics', Martinns Nighoff Publishers, The Hague, 1982
13 Haddaoui, N., Moet, A. and Chudnovsky, A. *Polymer* 1986, **27**, 1377
14 Bakar, M., *PhD Thesis*, Case Western Reserve University, Cleveland, Ohio (1986)